Photoassisted Fowler-Nordheim-like tunneling from passivated GaAs microcantilevers

D. Paget[*] and A. C. H. Rowe
Physique de la matière condensée, Ecole Polytechnique, CNRS, F-91128 Palaiseau, France

S. Arscott and E. Peytavit
Institut d'Electronique, de Microélectronique et de Nanotechnologie (IEMN), CNRS UMR8520, Avenue Poincaré, Cité Scientifique, F-59652 Villeneuve d'Ascq, France

(Received 22 July 2011; revised manuscript received 8 December 2011; published 6 March 2012)

We have investigated the mechanisms of photoelectron tunneling into gold from tipless, nitridized, gallium arsenide microcantilevers through thin polymers. A study of the tunnel bias, tunnel distance, and light excitation power dependence of the tunneling photo-current reveals the tunneling process to be Fowler-Nordheim like. Both the value of the dielectric constant and the sign of the tunneling photocurrent at low excitation power suggest the important role of polymer defects.

DOI: 10.1103/PhysRevB.85.113301 PACS number(s): 73.40.Gk, 73.40.Qv, 72.80.Le, 85.75.−d

While the relevant processes for electron transport in reverse-biased metal-insulator-structures have been identified as standard tunneling, Fowler-Nordheim (FN) tunneling[1,2] or hopping between defects in the insulator,[3] there are at least three types of systems for which a better understanding of this transport is the subject of active research: (i) tunneling between metals through polymer or organic layers,[4,5] both for fundamental investigations of molecular energy levels and for applications exploiting light emission from organic compounds (calculations and experiments reveal FN-like behavior governed by the localized energy levels of the polymer),[6] (ii) charge and spin injection in hybrid semiconductor-magnetic metal devices in the dark[7] or under light excitation,[8] and (iii) spin-polarized electron tunneling from optically pumped GaAs using a tunnel gap of adjustable width.[9,10]

In this work the tunneling mechanism for photoelectron transport from a GaAs microcantilever through a polymer and into a gold surface is investigated. Gold is chosen since it has an energy-independent density of states.[11] As shown in the inset of Fig. 1, the GaAs microcantilever, fabricated using an assembly technique developed by the authors,[12] is held at a distance d from the gold surface and is excited from the rear by a laser whose energy ($h\nu = 1.59$ eV) is close to the bandgap, E_g, of GaAs. By monitoring the position of the laser beam reflected from the cantilever, we ensure that all tunneling current measurements are made prior to mechanical contact. The tunnel gap between the GaAs and the gold is filled with low-viscosity (20 cSt), hydrophobic, polydimethylsiloxane (PDMS) by spin coating onto the heated metal surface (130 °C) in order to desorb all traces of water. The native oxide covering the GaAs cantilever is replaced by a monolayer of nitrogen using a recently developed hydrazine-sulfide treatment followed by annealing in an inert gas atmosphere at 500 °C.[13,14] The experimental setup and procedure have been described before.[15] After stabilization of the dark current ($I_{\rm dark}$) to a set current at a bias of $V_c = -1.5$ V, the feedback loop is opened and two bias scans are performed, one with the laser on and the second one in the dark. The difference between the measured currents is the tunneling photocurrent ($I_{\rm ph}$). Since relatively small set currents are used, both $I_{\rm dark}$ and $I_{\rm ph}$ are stable over a period of several hours.

The band structure of the metal-insulator-semiconductor structure is shown in Fig. 1. Optical excitation of photoelectrons from the rear face of the cantilever results in electron accumulation at the front face. Photoelectron tunneling takes place from a well-defined energy, $f\phi_b$, above the bottom of the GaAs conduction band, where ϕ_b is the surface barrier and f is the exponent of the excitation power dependence of $I_{\rm ph}$. At equilibrium, the surface Fermi level is usually considered to be pinned near midgap at the peak of the surface density of states, $N_S(\mathcal{E})$, yielding a surface barrier ϕ_0. However, light excitation and the application of a tunnel bias shift the Fermi level to a different, quasi-Fermi level for electrons, $E_{\rm Fe}$, that lies at an energy qV_s below the bulk value (V_s is the photovoltage and q is the negative electron charge) and at $\Delta\phi$ above the equilibrium position at the surface. As seen from Fig. 1, one has $\delta\phi_b = \phi_b - \phi_0 = \Delta\phi - qV_s$. The tunnel barrier height is determined by the lowest unoccupied molecular orbital (LUMO) of the PDMS. Spatial variations in the LUMO resulting from the electric field in the tunnel gap, as well as image charge effects, determine the distances d_1 and d_2 (see Fig. 1). Fowler-Nordheim tunneling occurs when $d_2 < d$.

Curves a to e in Fig. 2 show the bias dependencies of $I_{\rm ph}$ corresponding to set currents ranging between 0.88 and 3.17 nA. For curves a, b, and c, $I_{\rm ph}$ depends exponentially on tunnel bias, with a slope that diminishes with increasing set current. Curves e and d, and to some extent c, also show an inflexion point that reveals a distinct transport process at high bias. As shown in Fig. 3, this is particularly clear at lower light excitation power, P. The full power curve (a) (the same data as curve c of Fig. 2) is exponential for $V < -1.3$ V. For curves b, c, and d, corresponding to lower powers, a negative contribution progressively appears that gives rise to a change in sign of $I_{\rm ph}$. At the lowest power (curve e), $I_{\rm ph}$ is negative over the entire bias range.

This effect is not observed in the absence of the PDMS and can be given a simple qualitative explanation. Since $I_{\rm ph}$ is quite small compared with $I_{\rm dark}$ (curve g), one might expect that a part of $I_{\rm ph}$ is in fact a light-induced modulation ($\delta I_{\rm dark}$) of $I_{\rm dark}$ arising from the replacement of $\Delta\phi$, qV_s, and $\delta\phi_b$ by their values in the dark $\Delta\phi_d$, qV_{sd}, and $\delta\phi_{bd} = \Delta\phi_d - qV_{sd}$. As shown in Fig. 1, $I_{\rm dark}$ is due to electron tunneling into the

 ©2012 American Physical Society

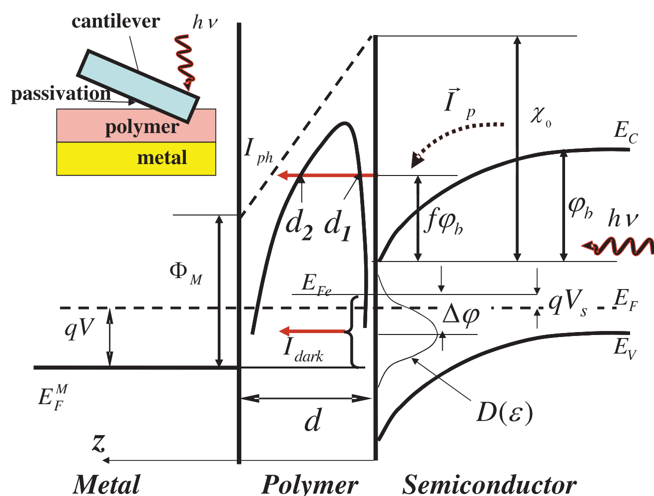

FIG. 1. (Color online) The inset shows a schema of the injection experiment. The main figure shows the band structure of the semiconductor/polymer/metal junction for a bias V applied to the metal. $I_{\rm ph}$ originates from photoelectrons at energy $f\phi_b$ above the bottom of the conduction band at the surface. Here qV_s is the photovoltage energy and $\Delta\phi$ represents the unpinning of $E_{\rm Fe}$ from its midgap position coinciding with the peak of $N_S(\mathcal{E})$. Also shown is the polymer LUMO in the tunnel gap without (dotted line) and with (solid line) image charge effects.

metal from semiconductor states situated above the metallic Fermi level and below $E_{\rm Fe}$. Qualitatively, illumination changes the electric field in the tunnel gap and V_{sd} is replaced by V_s. This is equivalent to an opposite change of V and implies that $\delta I_{\rm dark} \propto -(V_s - V_{sd})\partial I_{\rm dark}/\partial V$. Indeed, curve e corresponds very well with the bias derivative of $I_{\rm dark}$ (curve f). Modified curves (c′, d′, and e′) in Fig. 2, obtained by adding the quantity $V^*\partial I_{\rm dark}/\partial V$, where V^* is given in Table I, no longer exhibit the inflexion point. The inset of the figure shows the power dependence of the corrected photocurrent at $V = -1.5$ V and

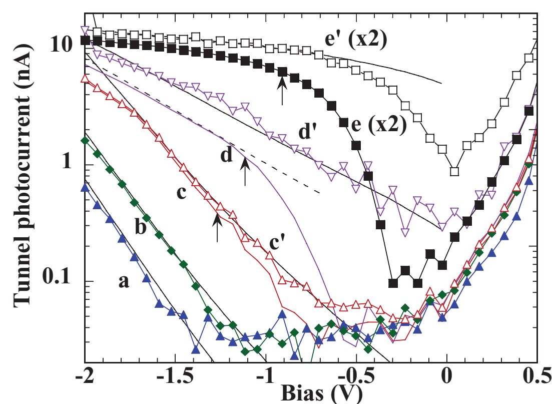

FIG. 2. (Color online) Bias dependence of $I_{\rm ph}$ for set currents in the dark of 0.88, 1.42, 1.92, 2.58, and 3.17 nA (curves a to e, respectively). Curves a and b are satisfactorily fitted by the model of Eqs. (3), (4), and (5) (solid lines). For curves c and d, satisfactory agreement can be reached below a threshold bias indicated by an arrow. Curves c′, d′, and e′ were obtained after removal of a negative contribution to the total tunnel photocurrent and correspond to a FN-like tunneling process.

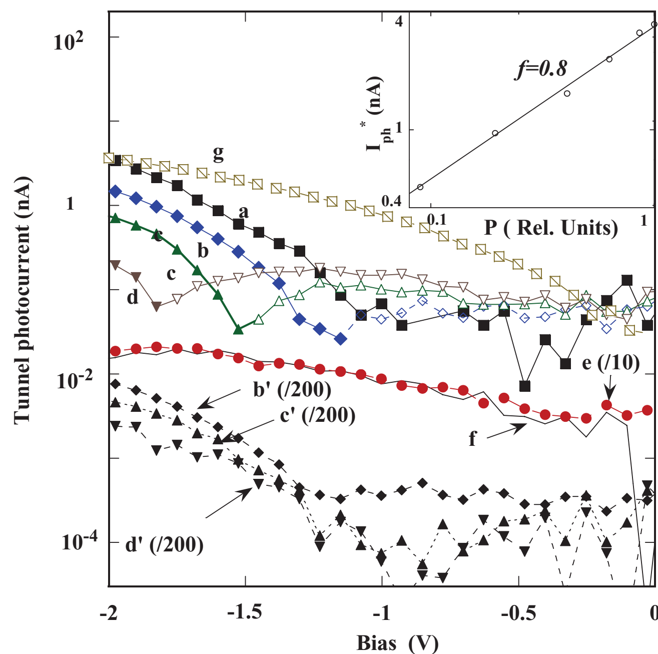

FIG. 3. (Color online) Bias dependence of $|I_{\rm ph}|$ for relative light excitation powers (curves a–e) of 1, 0.40, 0.19, 0.09, and 0.022. Curve a is the same data as curve c of Fig. 2. Curves b, c, d, and e exhibit negative tunnel photocurrents shown by dotted lines and open symbols. Also shown is $I_{\rm dark}$ (curve g), which is much larger than $I_{\rm ph}$. Its derivative as a function of bias (curve f) is close to curve e. After removal of this negative contribution, these curves become curves b′, c′, and d′, respectively (denoted $I^*_{\rm ph}$). The inset reveals a power-law dependence of $I^*_{\rm ph}$ on P (at $V = -1.8$ V) with $f = 0.8$.

reveals, as found elsewhere, a power-law dependence with exponent $f = 0.8$.[15]

In order to interpret the inflexion point, $I_{\rm dark}$ is considered equal to the Schottky current I_s,

$$K_d\rho_m \int_{qV+\delta\phi_{bd}}^{\Delta\phi_d} N_S(\mathcal{E})p(\mathcal{E})\,d\mathcal{E} = -I_0\exp(-\Delta\phi_d)[\exp(qV_{sd}/k_BT)-1], \quad (1)$$

where the tunnel probability $p(\mathcal{E})$ at the energy $\mathcal{E}$ with respect to midgap, is of the form $p^*(\mathcal{E})\exp[-d(qV+\delta\phi_{bd})/(2d_0\sqrt{\Phi_s^*})]$. $p^*(\mathcal{E})$ does not depend on $\delta\phi_{bd}$ or qV_{sd}. Here $d_0 = 0.13$ nm$/\sqrt{\rm eV}$ and $\Phi_s^* = (\Phi_m + \chi_0 + \phi_0)/2$. K_d is a constant and I_0 is the saturation current. Since the integrand is positive definite, a decrease in $\Delta\phi_d$ while keeping $\delta\phi_{bd}$ constant cannot interpret the results. Such a change implies a decrease of $I_{\rm dark}$ on the left-hand side of Eq. (1) but also an increase of the right-hand side. The experimental results rather

TABLE I. Parameter values used in the fits of Fig. 2.

	a	b	c(c′)	d(d′)	e′
d (nm)	1.37	1.27	1.10	0.55 (0.50)	0.05
ϵ	7	7	7	7	20
K	1	1	1	7.5×10^{-3} (4×10^{-3})	9×10^{-5}
V^* (V)	0	0	(0.03)	(0.60)	(0.80)

imply, as assumed by the above qualitative picture, an increase of $\delta\phi_{bd} = \Delta\phi_d - qV_{sd}$ due to an increase qV_{sd} that leads to a decrease of both $I_{\rm dark}$ and I_s.

The light-induced photovoltage alone can only induce a decrease of $\delta\phi_{bd}$ and cannot interpret the results. It is proposed here that $\delta I_{\rm dark}$ is rather due to light-induced modification of $N_S(\mathcal{E})$ which follow the semiconductor statistics while other states of density $N_M(\mathcal{E})$ are in equilibrium with the metal.[16] The efficient capture of photogenerated carriers at defects in the PDMS implies that more interface states follow the semiconductor statistics thereby increasing $N_S(\mathcal{E})$ and decreasing $N_M(\mathcal{E})$. Charge conservation reads[15]

$$\delta\phi_{bd}(C_m + C_s) - q^2 \int_{qV+\delta\phi_{bd}}^{0} N_M(\mathcal{E})\, d\mathcal{E} = -q^2 \int_0^{\Delta\phi_d} N_S(\mathcal{E})\, d\mathcal{E} - C_m qV, \qquad (2)$$

where C_m and C_s are the capacitances of the tunnel gap and of the surface depletion layer, respectively. Since the shapes of $N_S(\mathcal{E})$ and $N_M(\mathcal{E})$ are not well known, especially in the presence of defects in the polymer, it is beyond the scope of the present work to solve Eqs. (1) and (2) to determine quantitatively the effect of a change of $N_S(\mathcal{E})$ on $I_{\rm dark}$. Provided the second term of the left-hand side of Eq. (2) is not too large with respect to the first term, it can be qualitatively shown that the increase (decrease) of $N_S(\mathcal{E})$ [$N_M(\mathcal{E})$] is consistent with a decrease of qV_{sd} and a smaller decrease of $\Delta\phi_d$ such that I_s and $I_{\rm dark}$ both decrease.

In order to analyze the bias dependence of the corrected tunnel photocurrent, $I^*_{\rm ph}$, one writes

$$I^*_{\rm ph} = K\rho_m n_s D(E), \qquad (3)$$

where K is a constant and ρ_m is the metallic surface density of states. The photoelectron concentration n_s per unit area at the tunneling energy E depends on bias because of a possible bias dependence of the surface recombination velocity.[15] The probability $D(E)$ of the tunnel process is given by

$$D(E) = \exp\left[-\frac{2\sqrt{2m}}{\hbar}\int_{d_1}^{d_2}\sqrt{\chi^*(z)}\right]dz, \qquad (4)$$

where $\chi^*(z)$ is the tunnel barrier height at distance z from the semiconductor surface.

Assuming a normal tunneling process without image charge effects ($d_2 \approx d$) one finds that, to first order in qV/Φ^*_b, where $\Phi^*_b = \Phi^*_s - (E_G + 2f\phi_0)/2$, that $I^*_{\rm ph}$ should scale like $\exp[(4\Phi^*_b + qV)/qV_{\rm ph}]$ at large tunnel distance.[15] Here, $(qV_{\rm ph})^{-1} = -d/(2d_0\sqrt{\Phi^*_b})$, implying that the slope of the exponential dependence of the photocurrent on tunnel bias should decrease with distance.[15] Although this prediction is qualitatively in agreement with curves a, b, and c of Fig. 2, quantitative analysis shows that FN-like tunneling ($d_2 < d$) cannot be neglected. In particular, a comparison of the measured values of $V_{\rm ph}$ and the tunneling photocurrents between curve a and curve c yield $\Phi^*_n \approx 1$ eV. Using this value, one finds[2,15] that the threshold of the FN-like process without image charge effects, $qV^0_{\rm th} = -2\Phi^*_b + \chi_0$, lies within the experimental tunnel bias range. Moreover, image charge effects push $qV_{\rm th}$ even closer to zero, implying that FN-like tunneling must be taken into account.

A simplified FN-like model[1,2] cannot explain the results either. In order to calculate d_1 and d_2, this model assumes that the bias is larger than the tunnel barrier height and that the polymer dielectric constant ϵ is smaller than those of the metal (ϵ_m) and of the semiconductor (ϵ_s). Again, although reasonable agreement with the slopes of $I^*_{\rm ph}$ versus bias and of $qV_{\rm th}$ are obtained using a bias-independent value of n_s and a tunnel gap ranging from 0.2 to 0.7 nm, this can be achieved only with values of the PDMS relative permittivity $\epsilon \approx \epsilon_s$ and a bias comparable to the tunnel barrier height.

The shape of the tunnel barrier height for electrons at energy $f\phi_b$ above the bottom of the conduction band at the semiconductor surface is written more correctly as

$$\chi^*(z) = \chi_0 - f\phi_b + qV^* z/d + E_{im}(z), \qquad (5)$$

where $V^* = V - V_0$ and V_0 is related to the energy of the LUMO at the metal surface without image charge effects (Φ_m) by $V_0 = \chi_0 + E_G - \phi_b - \Phi_m$. The image charge potential $E_{im}(z)$ is now given by

$$E_{im}(z) = -\frac{q}{8\pi d\epsilon}\left[\frac{K_s d}{z} + \sum_{n=1}^{\infty} K_s^n K_m^{n-1}\left(\frac{d}{nd - z} + \frac{dK_s^2}{nd + z}\right) + \sum_{n=1}^{\infty}\frac{K_s^n K_m^n}{n}\right] \approx -\lambda\xi(z), \qquad (6)$$

where $K_s = (\epsilon - \epsilon_s)/(\epsilon + \epsilon_s)$ and $K_m = (\epsilon - \epsilon_m)/(\epsilon + \epsilon_m) \approx -1$[17] and $\lambda = q\ln(2)/(8\pi d\epsilon)$. One has $\xi(z) \approx -\frac{1.15d^2}{z(d-z)} + 0.124(K_s + 1)\exp[5.65(1 - z/d)]$, where the first term is the expression used by Simmons[1] who takes $K_s = -1$.

Shown in Fig. 2 is a fit of the bias dependencies using Eqs. (3) and (5) where numerical values of d_1 and d_2 are obtained by setting $\chi^*(z) = 0$. Apart from the parameters given in Table I, from $f = 0.8$ as suggested by the inset shown in Fig. 3, $\chi_0 = 2$ eV and $\Phi_m = 3.25$ eV, all other parameter values are the same as in Ref. 15. The value of Φ_m is determined by the band lineup between the metal and the polymer and is found to be smaller than the gold work function used in Ref. 15 by 2 eV.

For curves a, b, c′, and d′ the fit using identical parameters values is very satisfactory. The bias dependence of $I^*_{\rm ph}$ is dominated by that of $D(E)$ since, at large tunnel distance, n_s is bias independent. In contrast, for curve e′ it is necessary to increase the effective dielectric constant of the tunnel gap, possibly because the nitride layer makes a more significant contribution to the effective dielectric constant or because of residual traces of water at the metal surface. Since the tunnel distance is small, the bias dependence of $I^*_{\rm ph}$ is dominated by that of n_s, so an accurate fit now depends on semiconductor surface parameters such as the width and amplitude of the distribution of surface states and the surface recombination velocity. A convincing interpretation of curve e′ cannot, therefore, be performed reliably by varying all these parameters and was not attempted. For curve e′ and, to some extent curve d′, the tunneling photocurrent is reduced relative to the other set currents as seen from the relative values of K

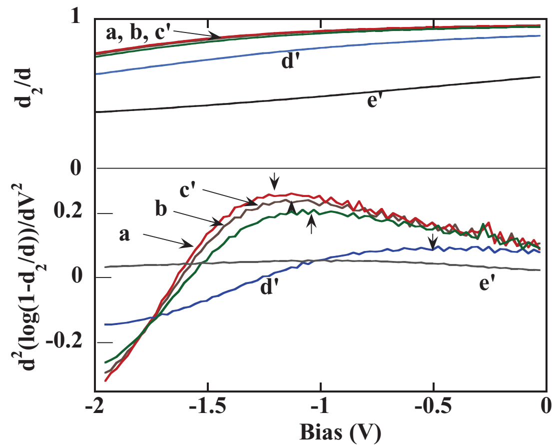

FIG. 4. (Color online) The top panel shows the calculated bias dependence of d_2/d for the curves of Fig. 2. In order to find the inflexion points of these curves, the bottom panel shows the second bias derivative of $\log(1 - d_2/d)$. For each curve the estimated thresholds for FN injection are shown by arrows.

given in Table I. It is proposed that this reduction arises because the tunnel gap becomes comparable with the roughness of the cantilever.[18] In this case, the tunnel current will mostly originate from the regions of smallest tunnel gap, thereby reducing K.

In order to demonstrate the relevance of the FN-like process, the top panel of Fig. 4 shows the calculated bias dependencies of d_2/d. The ratio is close to unity at zero bias and decreases with increasing negative bias and the values for curves a, b, and c′ are quite similar. An estimate of the threshold of the FN process is found by calculating the inflexion point of the bias dependence of log $(1 - d_2/d)$. For curve a of Fig. 2, the estimated threshold is -1.2 V, slightly smaller than the measured onset of $I^*_{\rm ph}$ possibly due the limited sensitivity of the current measurement. For curve b, the two bias values are similar, while, for curve c, a normal tunneling process cannot be excluded for absolute biases larger than about 1 V.

It is concluded that elastic tunneling through the PDMS is the current-limiting process. The main reason for the relevance of FN-like tunneling through the polymer and for normal tunneling in its absence is probably the reduction of the work function due to the polymer, which reduces the threshold voltage of the FN-like tunneling. The analysis reveals the role of polymer defects for tunneling of photoelectrons between a semiconductor and a metal. Charged defects in the polymer are responsible both for the negative tunnel photocurrent and probably also for the large dielectric constant.[19] At the present stage, it is not possible to conclude whether the FN-like tunneling barrier is determined by the PDMS LUMO or, as considered in Ref. 6, by a localized defect of lower energy. In any case, the only apparent effect of discrete LUMO states is to change the exact value of the threshold voltage.[5]

*daniel.paget@polytechnique.edu

[1] J. G. Simmons, J. Appl. Phys. **34**, 1793 (1963).
[2] A. C. H. Rowe and D. Paget, Phys. Rev. B **75**, 115311 (2007).
[3] S. Hasannli, N. Mursakulov, U. Samedova, N. Abdulzade, B. Mamedov, and R. Guseynov, Semiconductors **44**, 875 (2010).
[4] J. M. Beebe, B. S. Kim, J. W. Gadzuk, C. D. Frisbie, and J. G. Kushmerick, Phys. Rev. Lett. **97**, 026801 (2006).
[5] M. Araidai and M. Tsukada, Phys. Rev. B **81**, 235114 (2010).
[6] T. Ouisse, Eur. Phys. J. B **22**, 415 (2001).
[7] Y. J. Park, M. C. Hickey, M. J. Van Veenhuizen, J. Chang, D. Heiman, and J. S. Moodera, Phys. Rev. B **80**, 245315 (2009).
[8] Y. Park, M. Hickey, M. Van Veenhuizen, J. Chang, D. Heiman, C. Perry, and J. Moodera, J. Phys. Condens. Matter **23**, 116002 (2011).
[9] D. T. Pierce, Phys. Scr. **38**, 291 (1988).
[10] D. Vu, H. F. Jurca, F. Maroun, P. Allongue, N. Tournerie, A. C. H. Rowe, D. Paget, S. Arscott, and E. Peytavit, Phys. Rev. B **83**, 121304 (2011).
[11] D. Papaconstantopoulos, *Handbook of the Band Structure of Elemental Solids* (Plenum Press, New York, 1986).
[12] S. Arscott, E. Peytavit, D. Vu, A. C. H. Rowe, and D. Paget, J. Micromech. MicroEng. **20** (2010).
[13] V. Berkovits, D. Paget, A. Karpenko, V. Ulin, and O. Tereshchenko, Appl. Phys. Lett. **90**, 022104 (2007).
[14] V. Berkovits, V. Ulin, O. Tereshchenko, D. Paget, A. Rowe, P. Chiaradia, B. Doyle, and S. Nannarone, J. Electrochem. Soc. **158**, D127 (2011).
[15] D. Vu, S. Arscott, E. Peytavit, R. Ramdani, E. Gil, Y. André, S. Bansropun, B. Gérard, A. C. H. Rowe, and D. Paget, Phys. Rev. B **82**, 115331 (2010).
[16] H. Card and E. Rhoderick, J. Phys. D: Appl. Phys. **4**, 1589 (1971).
[17] M. Desjonquères and D. Spanjaard, *Concepts in Surface Physics* (Springer-Verlag, Berlin, 1996).
[18] The area of the tunnel injection is not well known for the present tipless cantilevers. However, it has been found that AFM imaging can be performed with a resolution comparable to that of commercial silicon tips, implying that the tunnel area is not much larger than that obtained with a tip. As seen in the inset of Fig. 1, this result is probably caused by the sharp end of the cantilever due to faceting.
[19] J. Mark, *Polymer Data Handbook* (Oxford University Press, Oxford, 1999).